Sparse Interference Pre-Cancellation for FTN-OQAM Systems

Naila Lahbabi, Hao Lin, Charbel Abdel Nour, Catherine Douillard, Pierre Siohan

Sparse Interference Pre-Cancellation for FTN-OQAM Systems

Naila Lahbabi*&, Hao Lin*, Charbel Abdel Nour&, Catherine Douillard&, Pierre Siohan†
* Orange Labs, Cesson Sévigné, France.
& Télécom Bretagne, Brest, France.
† retired from Orange Labs

***Abstract*—In this paper, we propose several precoding methods to reduce the interference caused by Faster-Than-Nyquist (FTN) signaling for Orthogonal Frequency Division Multiplexing Offset Quadrature Amplitude Modulation (OFDM/OQAM). The proposed precoders are combined with an FTN-OFDM/OQAM modulator to pre-cancel the interference at the transmitter side. An iterative receiver for each precoding scheme is also presented. With the simulations, we show that the convergence speed of the FTN-OFDM/OQAM transceiver increases with the proposed precoders.**

I. Introduction

Although OFDM has been widely used in radio communications, the issue of whether it should be the ultimate waveform for future radio systems such as 5Ghas recentlytriggered
many discussions [1] and is still open. The main drawbacks of OFDM have long been identified i.e., overhead wasting due to cyclic prefix (CP) insertion and weak robustness against frequency dispersive channels. Among the competing waveforms proposed to overcome these drawbacks, the offset signaling on the top of OFDM (known as OFDM/OQAM) is recognized as a good alternative candidate to OFDM [2] because of two advantages. First, OFDM/OQAM systems have the flexibility of using different waveforms. Actually this advantage is due to its offset signaling [3]. Second, due to the improved waveform, the use of CP is not always necessary, which keeps a full Nyquist rate [2], [4], [5]. Moreover, in [6], the link to the filter bank approach is first established, proving that the OFDM/OQAM, or OQAM in short, systems can efficiently be realized with Fast Fourier Transform (FFT) and polyphase filtering, which further justifies their practical feasibility. Thus, the OQAM is sometimes also called Filter Bank Multi-Carrier (FBMC) [5].

The continuous increasing mobile data volume constrains the future radio systems to include advanced modulations/waveforms offering higher data rates with more efficient bandwidth usage. One possibility is to violate the well-known Nyquist condition [7] by transmitting faster than the Nyquist rate, i.e. using a technique also known as FTN signaling. The original idea was raised by Mazo in 1975 [8]. He stated that the transmission rate is not necessarily limited by the Nyquist rate, meaning that faster transmission rate can be envisaged provided that interference is accepted. Mazo also showed that as long as the boosted transmission rate does not go beyond 1.25x[1], the resulted minimum sequence distance keeps constant, thus not entailing any performance degradation, provided the receiver uses Maximum Likelihood Sequence Estimation (MLSE) [9]. However, this scheme was not deemed attractive until the arrival of the mobile data tsunami became unavoidable. The combination of FTN with OFDM [10] made this scheme even more interesting.

The first work on the combination of OQAM and FTN, denoted here as FTN-OQAM, was reported in [12]. The authors modified the classical OQAM of [6] by inserting a block named *FTN mapper* between the OQAM modulator and the FFT. Due to this additional block, the complexity of their solution is higher than that of the classical OQAM system and depends on the block size. An iterative Maximum A Posteriori (MAP)-based receiver, whose complexity increases with the modulation order, is proposed in [13]. Later, the implementation of FTN-OQAM was revised in [14]. The proposed algorithm is able to approach very closely the promised performance of FTN systems without complexity increase compared to a classical OQAM system. At the receiver side, a Minimum Mean Square Error Linear Equalization and Interference Cancelation (MMSE LE-IC) was introduced. Unlike the MAP-based receiver, the MMSE LE-IC algorithm is independent of the modulation order which makes it a good candidate if high modulation orders are to be used.

In this paper, we consider an FTN-OQAM transmission system with iterative processing at the receiver side and aim to improve the iterative receiver convergence while keeping its complexity under an acceptable level. The proposed method involves combining a precoder with FTN-OQAM in order to pre-cancel the interference introduced by FTN signaling at the transmitter side. Given the nature of this interference, we propose a sparse precoding pattern. Actually, interference pre-cancellation is only applied to a group of symbols positions in the transmitted block while keeping the original OQAM symbols at the other positions. At the receiver side, we propose a two-step MMSE LE-IC algorithm. First, the precoded symbols are detected and used to reduce their interference with the non-precoded symbols. Then these latter symbols are detected and used, at the next iteration, to remove their interference with the precoded symbols.

The reminder of the paper is organized as follows. Sec-

[1] A ratio between Nyquist rate and FTN rate.

tion II introduces the background of FTN-OQAM as well as the transceiver presented in [14]. Section III describes our proposed precoding methods, while in Section IV, their performance is evaluated and compared to [14]. Conclusions are given in Section V.

II. OQAM AND FTN-OQAM

In this section, we briefly present the background of OQAM and its combination with FTN.

A. OQAM

For M subcarriers, the continuous-time OQAM signal in baseband is [6]:

$$s(t) = \sum_{m=0}^{M-1} \sum_{n=-\infty}^{+\infty} a_{m,n} \underbrace{g(t - \frac{nT_0}{2}) e^{j2\pi m F_0 t} e^{j\Phi_{m,n}}}_{g_{m,n}(t)}, \quad (1)$$

and the equivalent baseband discrete-time OQAM signal is [6]:

$$s[k] = \sum_{m=0}^{M-1} \sum_{n\in\mathbb{Z}} a_{m,n} g[k - nN] e^{\frac{j2\pi m(k-\frac{D}{2})}{M}} e^{j\Phi_{m,n}}. \quad (2)$$

The pulses $g_{m,n}$ are called basis functions and construct a Hilbert basis, with $T_0F_0 = 1$, where T_0 is the symbol duration and F_0 is the subcarrier spacing. $g(t)$ is a prototype function of length L (without any restriction, we suppose $L = bM, b \in \mathbb{N}$), $N = \frac{M}{2}$ is the discrete time offset, $D = L - 1$ and $\Phi_{m,n}$ is a phase term often equal to $\frac{\pi}{2}(m + n) + \Phi_0$, where $\Phi_0 = 0$ or $\pm\pi mn$. The real-valued transmitted symbol $a_{m,n}$ on the m^{th} subcarrier at time instant n is obtained from taking the real and imaginary part of the complex-valued 2^{2K}-QAM constellation. The orthogonality constraint of OQAM is expressed using the real inner product as:

$$\Re\left\{\int_{-\infty}^{+\infty} g_{m,n}(t) g^*_{m',n'}(t) dt\right\} = \delta_{m,m'}\delta_{n,n'}, \quad (3)$$

where, δ is the Kronecker symbol. It is worthwhile noting that this orthogonality condition can only be satisfied at the Nyquist rate $T_0F_0 = 1$ or above.

B. FTN-OQAM

The FTN-OQAM modulator consists in packing the pulses closer in time at a signaling rate faster than permitted by the Nyquist transmission criterion. The modulated baseband signal is expressed as [14]:

$$s(t) = \sum_{m=0}^{M-1} \sum_{n=-\infty}^{+\infty} a_{m,n} g(t - n\tau\frac{T_0}{2}) e^{j2\pi m F_0 t} e^{j\Phi_{m,n}}, \quad (4)$$

where $0 < \tau < 1$ is the FTN time packing factor. The discrete-time signal is obtained:

$$\begin{aligned} s[k] &= \sum_{m=0}^{M-1} \sum_{n=-\infty}^{+\infty} a_{m,n} g[k - nN_f] e^{\frac{j2\pi mk}{M}} e^{j\Phi_{m,n}} \quad (5) \\ &= \sum_{m=0}^{M-1} a_{m,n} e^{\frac{j2\Pi mk}{M}} e^{j\Phi_{m,n}} \sum_{n=-\infty}^{+\infty} g[k - nN_f], \end{aligned}$$

where, $T_s = \frac{T_0}{M}$ is the sampling rate, $F_0 = \frac{1}{MT_s}$ and M is the size of IFFT/FFT.

N_f is called the FTN factor and is defined as $N_f = \lfloor \tau.\frac{M}{2} \rfloor$, where $\lfloor . \rfloor$ denotes the floor function.

At the receiver side, the signal is detected using an MMSE LE-IC iterative based algorithm. The number of iterations for the system convergence depends on the FTN packing factor and on the modulation order. In order to reduce the number of iterations while keeping the same complexity as the FTN-OQAM system, we combine a precoder with the FTN-OQAM modulator. The idea behind is to pre-cancel the known interference at the transmitter side so that less iterations are needed.

III. SPARSE INTERFERENCE PRE-CANCELLATION (SIPC) METHOD

In this section, we present the SIPC method for pre-canceling the Inter-Symbol-Interference (ISI) and Inter-Carrier-Interference (ICI) at the transmitter side using the transceiver in [14].

At the demodulator output, the received signal at frequency m_0 and time instance n_0 is:

$$\begin{aligned} y_{m_0,n_0} &= \Re(\sum_k s[k] g[k - n_0N_f] e^{-j\Phi_{m_0,n_0}} e^{\frac{-j2\pi m_0(k-\frac{D}{2})}{M}}) \\ &= a_{m_0,n_0} + \Re(\sum_{(m,n\neq n_0)} a_{m_0,n} e^{j\frac{\pi}{2}(n-n_0+m-m_0)} \quad (6) \\ &\quad \times \sum_k g[k - nN_f] g[k - n_0N_f] e^{\frac{j2\pi(k-\frac{D}{2})(m-m_0)}{M}}) \end{aligned}$$

The first term of (6) is the useful signal and the second term represents the added interference composed of ISI and ICI, which are expressed as:

$$\begin{aligned} ISI &= \sum_{q=-l,q\neq 0}^{+l} a_{m_0,n_0+q} \quad (7) \\ &\quad \underbrace{\times \Re(e^{j\frac{\pi}{2}q} \sum_k g[k - (n_0 + q)N_f] g[k - n_0N_f])}_{h_q} \end{aligned}$$

and

$$ICI_{n_0} = \sum_{p=-l',p\neq 0}^{+l'} \sum_{q=-l}^{l} a_{m_0+p,n_0+q} \times g^R_{p,q,n_0} \quad (8)$$

where h_q is the coefficient of the equivalent channel of ISI and

$$\begin{aligned} g^R_{p,q,n_0} &= \Re(e^{j\pi(\frac{2p(k-\frac{D}{2})}{M} + \frac{p+q}{2})} \quad (9) \\ &\quad \times \sum_k g[k - (n_0 + q)N_f] g[k - n_0N_f]) \end{aligned}$$

is the ICI contribution of symbols at positions (m_0+p, n_0+q) to the symbol at (m_0, n_0), with $p, q \in \mathbb{Z}$. ICI depends on the time instance n. Factors l and l' represent the zone of symbols contributing to ISI and ICI, respectively. They depend on the prototype filter and on the packing factor τ.

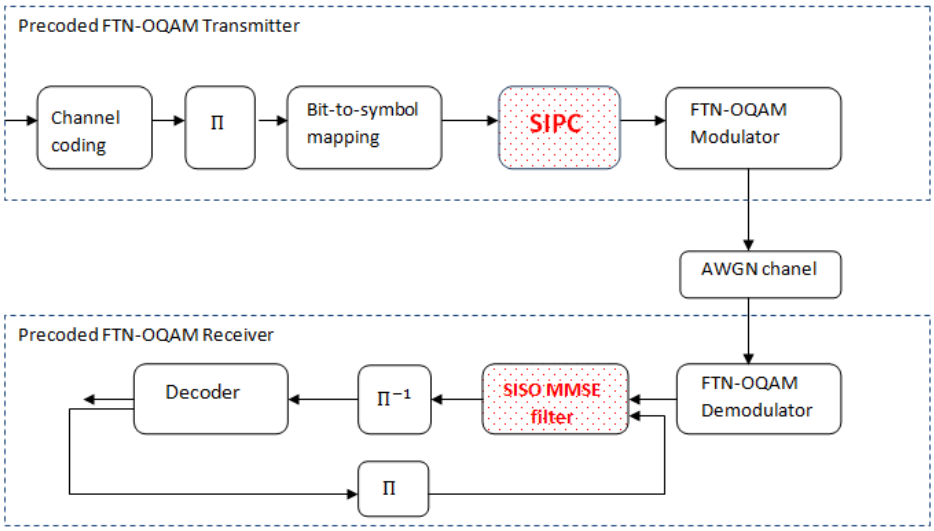

Fig. 1: The proposed precoded FTN-OQAM transceiver in the transmission chain of [14]. Dashed blocks are related to the SIPC method.

Since the ISI and ICI are known by the transmitter, they can be pre-canceled from OQAM symbols as follows:

$$c_{m,n} = a_{m,n} - ISI - ICI_n \tag{10}$$

Precoding the symbols at positions $(m+p, n+q)$ with $(p,q) \in [-l', l'] \times [-l, l]$ creates a different interference from the one used to precode the symbol at position (m,n). To overcome this problem, we propose a SIPC method which aims at removing the interference from only a group of symbol positions in the transmitted block. This group is determined according to the packing factor τ and the prototype filter. Moreover, two factors α and β $(0 \leq \alpha, \beta \leq 1)$ are introduced in order to control the amount of interference to be pre-canceled.

In the following, we propose three variations of SIPC precoders.

A. SIPC at time axis

In this section, a technique aiming at pre-canceling ISI at the transmitter, named SIPC from time axis (SIPC-t) is detailed. As shown in figure 1, the information bits are first encoded, interleaved and then mapped to OQAM symbols. According to the value of l, the block SIPC precodes symbols in positions n, as follows:

$$c_{m,n} = a_{m,n} - \alpha \left(\sum_{k=-l, l\neq 0}^{l} h_k a_{m,n-k} \right), \tag{11}$$

if $(n = k \ mod \ (l+2))$ or $(n = (k+1) \ mod \ (l+2))$, with $(k \in \mathbb{N}, k \leq l+1)$ and mod is the modulo operator.

The other positions in the transmitted block are not precoded and contain OQAM symbols. The precoding pattern is illustrated in figure 2, in case of $l = 2$, using a time-frequency lattice of the transmitted block. Because OQAM extracts only the real part of the received signal, symbols at odd positions do not contribute to ISI. Therefore, we alternate two precoded symbols and two OQAM symbols.

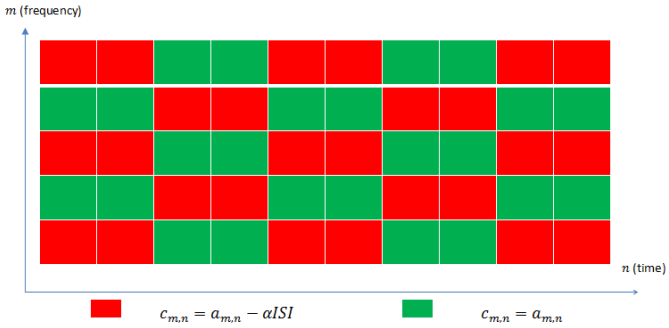

Fig. 2: The time-frequency lattice of the transmitted block. The red and green positions represent the precoded symbols and the non-precoded ones, respectively.

The two-step turbo-based MMSE-LE-IC receiver is illustrated in figure 3. At the first iteration, the precoded symbols are equalized using an MMSE-LE filter from the time axis (MMSE-t). Then, they are decoded by a Max-Log-MAP decoder. A soft estimation of these symbols, at the decoder's output, is used by the Soft-Interference-Cancellation (SIC 1) block to remove their interference with the non-precoded symbols. They are then equalized and decoded. At the next iteration, the soft estimation of the non-precoded symbols enables the block SIC 2 to cancel their interference with the precoded symbols and to update the MMSE-t coefficients.

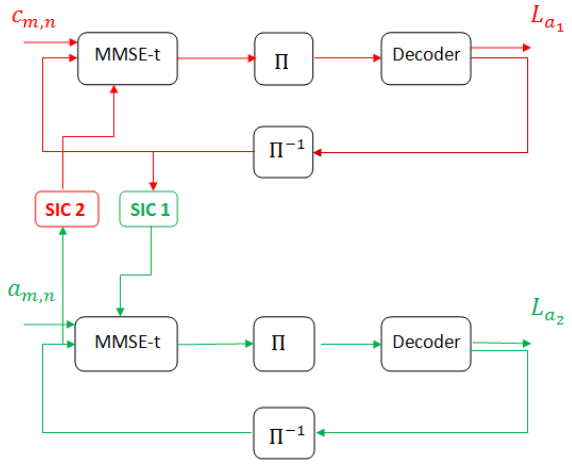

Fig. 3: Structure of the SISO MMSE LE-IC used for SIPC-t.

B. SIPC at frequency axis

The SIPC-t precoder can be replaced by a precoder operating in the frequency axis, named SIPC from frequency axis (SIPC-f), which pre-cancels ICI from symbols at frequency positions m, as follows:

$$c_{m,n} = a_{m,n} - \beta \left(\sum_{p=-l',p\neq 0}^{l'} \sum_{q=-l}^{l} a_{m_0+p,n_0+q} g_{p,q,n} \right), \quad (12)$$

if $(m = k \ mod \ (l^{'}+1)$, with $k \in \mathbb{N}, k \leq l^{'})$.

At the other positions, OQAM symbols are kept unchanged. Figure 4, presents an example of precoding pattern for $l^{'} = 1$. At the receiver side, we use a similar two-step turbo-based

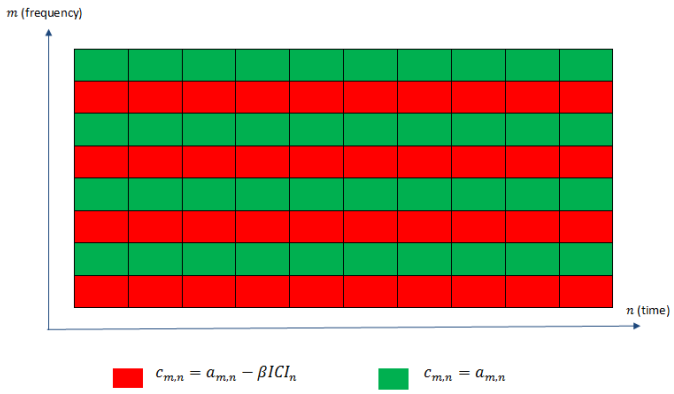

Fig. 4: The time-frequency lattice of the transmitted block. The red and green positions represent the precoded symbols and the non-precoded ones, respectively.

MMSE LE-IC algorithm as in the previous section. Since ICI depends on time, we choose to equalize the non-precoded symbols using a frequency domain MMSE LE (MMSE-f) equalization.

C. SIPC at both time-frequency axes

Now, we replace the SIPC block by a precoder to pre-cancel ISI and ICI from a group of symbol positions(m, n), named SIPC-tf, as follows:

$$c_{m,n} = a_{m,n} - \alpha \left(\sum_{k=-l,l\neq 0}^{l} h_k a_{m,n-k} \right) - \beta \left(\sum_{p=-l',p\neq 0}^{l'} \sum_{q=-l}^{l} a_{m_0+p,n_0+q} g_{p,q,n} \right), \quad (13)$$

if $(m_0 = k \ mod \ (l^{'}+1)$, with $k \in \mathbb{N}, k \leq l)$ and $(n_0 = k^{'} \ mod \ (l^{'}+2)$ or $n_0 = (k+1) \ mod \ (l^{'}+2)$ with $k^{'} \in \mathbb{N}, k^{'} \leq l^{'}+1)$. Figure 5 shows the precoding pattern in case of $(l, l^{'}) = (1, 2)$.

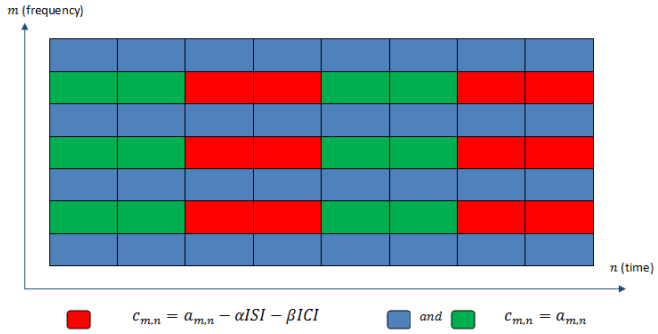

Fig. 5: The time-frequency lattice of the transmitted block. The red positions represent the precoded symbols while the green and blue positions represent the non-precoded symbols.

The turbo-based MMSE LE-IC receiver is illustrated in figure 6. At the first step, we equalize the precoded symbols in red positions using an MMSE-t filter. Then, their soft estimation at the decoder's output is used by block SIC2 to remove their interference with the non-precoded symbols in the green positions. At the second step, the symbols in the green positions are equalized using an MMSE-t filter. At the third step, the block SIC 3 uses the soft estimation of the red and green symbols to remove their interference with the blue ones. These symbols are then equalized using an MMSE-f filter. At the next iteration, the block SIC 1 uses the soft estimation of the blue symbols to remove their interference with the red ones.

IV. Simulations

In this section, we evaluate the Bit-Error-Rate (BER) of the proposed SIPC precoders using different pulse shapes, modulation orders and packing factors. Then, we compare the selected precoders to the FTN-OQAM system [14] in terms of BER performance.

A. SIPC precoders performance

We use a (1,5/7) Recursive Systematic Convolutional (RSC) code for channel coding with a size-15360 random interleaver, QPSK-Gray mapping, a MAP-based outer decoder and an

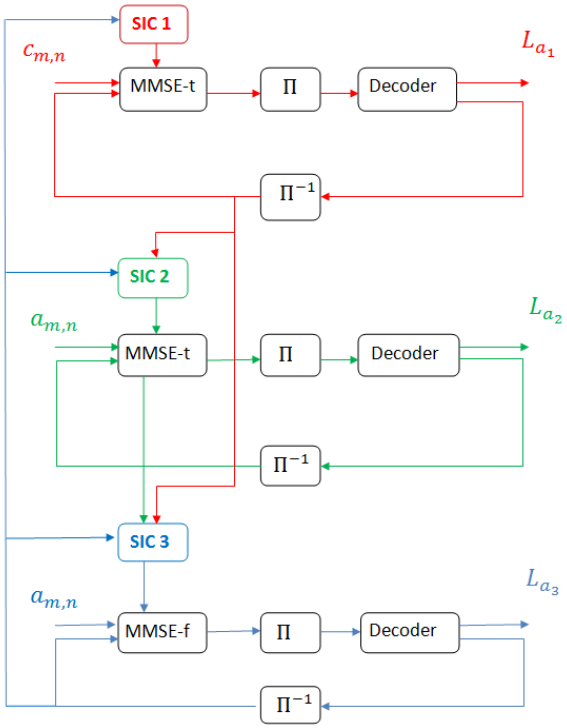

Fig. 6: Structure of the SISO MMSE LE-IC used for SIPC-tf.

MMSE filter of length 30 and delay 15. We compare the performance of the various SIPC precoders using different pulse shapes: PHYDYAS filter [15], Frequency Selective (FS) filter [4], Time Frequency Localization (TFL) filter [4], Isotropic Orthogonal Transform Algorithm (IOTA) filter [2], Extended Gaussian Function (EGF) filter with a spreading factor of 2 [6], and Square Root Raised Cosine filter with a roll-of factor of 0.5 (SRRC05) and a roll-of factor of 0.3 (SRRC03).

Figure 7 gives the result for SIPC-t at iteration 9. In what follows, SIPC-t results are given for $l = 2$. We observe that, the IOTA, TFL and EGF pulses give the best performance in terms of BER .

Table I summarizes the recommended pulse shapes for each SIPC precoder, modulation order and packing factor. SIPC-f-freq is similar to SIPC-f except that the MMSE-f filter is used for both the precoded and the non-precoded symbols. In the following, we choose $(l, l') = (2, 1)$ for SIPC-f, SIPC-tf and SIPC-f-freq.

Table II gives the selected SIPC method for each modulation order and packing factor, obtained from the comparison of the BER performance of these precoders.

B. Study of the effect of SIPC precoding on the FTN-OQAM transmission scheme

In this section, we show the effect of SIPC method on the FTN-transceiver in [14]. We keep the same configuration as in the previous section. Figure 8 gives the BER performance of both systems using QPSK modulation and $\tau = 0.5$. We observe that SIPC precoding improves the convergence of the iterative receiver: at SNR of 7 dB, SIPC-t precoding permits convergence at iteration 5, while the FTN-OQAM system only converges at iteration 7.

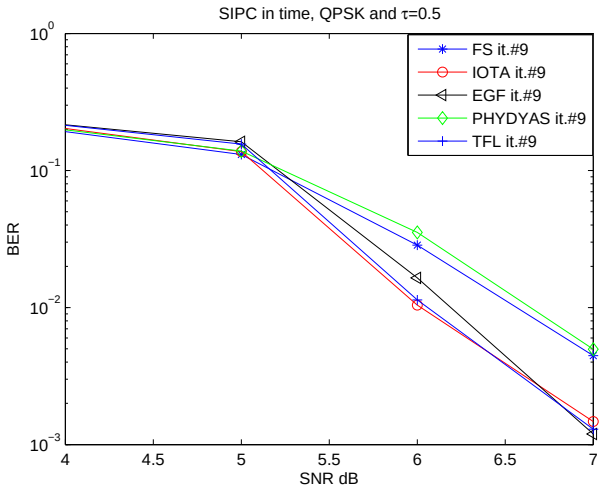

Fig. 7: BER evaluation for SIPC-t using different pulse shapes.

Precoder	QPSK	16-QAM	16-QAM	64-QAM	64-QAM
Packing factor (τ)	0.5	0.7	0.8	0.8	0.9
SIPC-t	TFL IOTA EGF	FS Phydyas IOTA	FS Phydyas IOTA	FS Phydyas	FS Phydyas SRRC05
SIPC-f	EGF TFL	IOTA FS Phydyas	FS Phydyas IOTA	FS Phydyas SRRC05	FS Phydyas SRRC05
SIPC-tf	TFL EGF IOTA	TFL	FS Phydyas	FS Phydyas	FS Phydyas IOTA
SIPC-f -freq	IOTA	FS Phydyas SRRC05	FS Phydyas SRRC05 SRRC03	FS Phydyas SRRC05 SRRC03	SRRC05 FS Phydyas

TABLE I: Recommended pulse shapes for the SIPC precoders.

Figure 9 gives the BER performance of both systems using 16QAM modulation and $\tau = 0.8$. We observe that SIPC precoding improves the convergence of the iterative receiver: SIPC-t precoding permits convergence at iteration 3 while the FTN-OQAM system only converges at iteration 7. We observe the same tendency in figure 10 for 64QAM modulation and $\tau = 0.9$: SIPC-f-freq precoding permits convergence at iteration 3 while the FTN-OQAM system only converges at iteration 5.

V. Conclusion

In this paper, we introduced a family of precoders, named SIPC, to deal with the interference caused by FTN signaling. Since this interference is known at the transmitter side, it can be pre-canceled before transmitting the signal. We introduced a precoding pattern depending on the used prototype filter and on the FTN packing factor. Monte Carlo simulations confirmed that the proposed method enables the FTN-OQAM system to converge with less iterations. The suitable pulse shapes for each SIPC method and modulation order were recommended.

Modulation order	Recommended SIPC precoders	Recommended pulses
QPSK ($\tau = 0.5$)	SIPC-t	TFL
	SIPC-tf	TFL
	SIPC-f-freq	IOTA
16QAM ($\tau = 0.7$)	SIPC-f-freq	FS
16QAM ($\tau = 0.8$)	SIPC-t	FS
	SIPC-t	Phydyas
64QAM ($\tau = 0.8$)	SIPC-t	Phydyas
	SIPC-f	Phydyas
	SIPC-tf	Phydyas
64QAM ($\tau = 0.9$)	SIPC-t	FS
	SIPC-t	Phydyas
	SIPC-f-freq	SRRC05

TABLE II: Recommended SIPC precoders and pulse shapes for different modulation orders and packing factors.

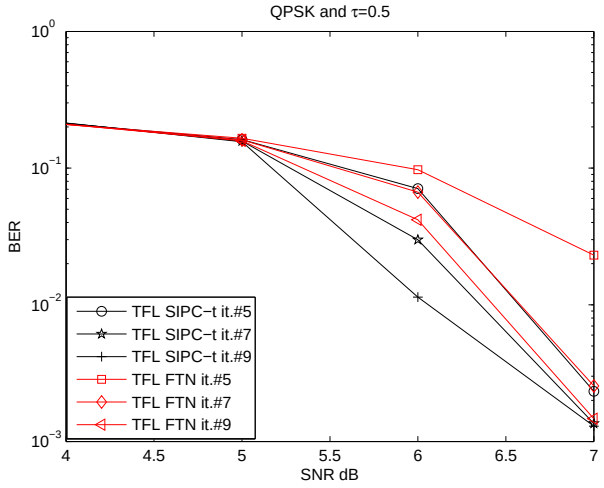

Fig. 8: BER evaluation for SIPC-t and the FTN-OQAM system using QPSK and $\tau = 0.5$.

Furthermore, the best precoders, in terms of BER performance, and their corresponding pulse shapes were also reported for each modulation order.

REFERENCES

[1] *"Mobile and Wireless communications enablers for the twenty-twenty information society"*.https://metis2020.com/.

[2] B. Le Floch, M. Alard, and C. Berrou.*"Coded Orthogonal Frequency Division Multiplex"*.Proceedings of the IEEE, vol. 83, pp. 982-996, June 1995.

[3] H. Bölcskei,*"Advances in Gabor Analysis"*. Chapter Orthogonal frequency division multiplexing based on offset QAM, pp. 321-352, 2003.

[4] D. Pinchon, P. Siohan, and C. Siclet.*"Design techniques for orthogonal modulated filterbanks based on a compact representation"*. IEEE Trans. Signal Process, vol. 52, no. 6, pp. 1682-1692, 2004.

[5] *"Physical Layer for Dynamic Spectrum Access and Cognetive Radio"*. http://www.ict-phydyas.org/index.php/camax/page/view?id=21.

[6] P. Siohan, C. Siclet and N. Lacaille.*"Analysis and design of OFDM/OQAM systems based on filterbank theory"*. IEEE Trans. Signal Process, vol. 50, no. 5, pp. 1170-1183, 2002.

[7] H. Nyquist.*"Certain topics in teleraph transmission theory"*.Trans. AIEE, vol. 47, pp.617-644, Apr. 1928.

[8] E. Mazo. *"Faster-Than-Nyquist signaling"*. Bell. Syst. Tech. Journal, 54:1451-1462, 1975.

[9] G. Forney. *"Maximum-likelihood sequence estimation of digital sequences in the presence of ontersymbol interference"*. Information Theory, IEEE Trans, vol. 18, no. 3, pp. 363-378, 1972.

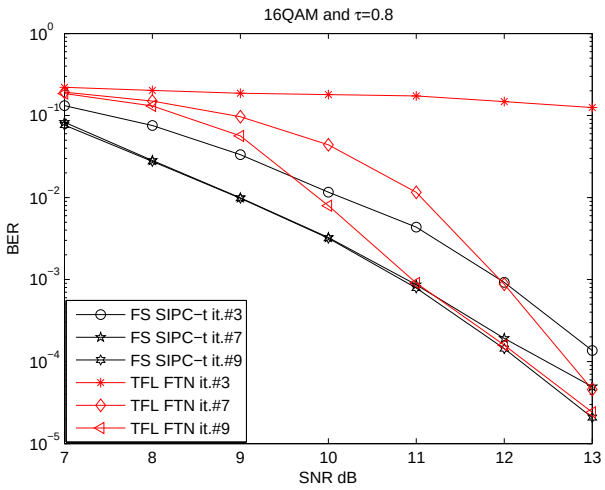

Fig. 9: BER evaluation for SIPC-t and the FTN-OQAM system using 16QAM and $\tau = 0.8$.

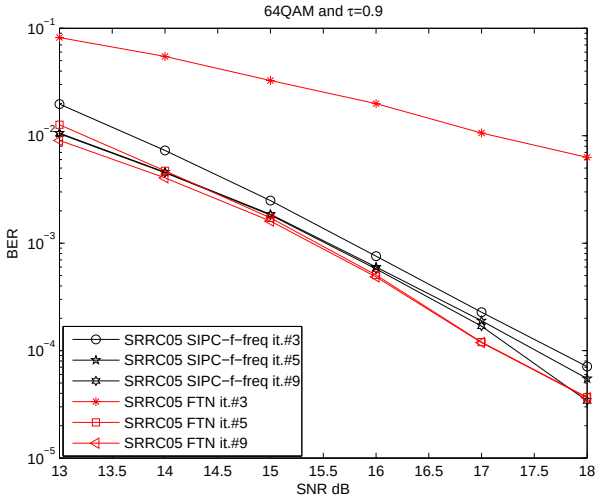

Fig. 10: BER evaluation for SIPC-f-freq and the FTN-OQAM system using 64QAM and $\tau = 0.9$.

[10] J.B. Anderson and F. Rusek. *"Improving OFDM: Multistream Faster-Than-Nyquist Signaling"*. In Turbo Codes Related Topics; 6th International ITG-Conference on Source and Channel Coding (TURBOCODING), 2006 4th International Symposium, pp. 1-5, Apr. 2006.

[11] F. Rusek and J.B. Anderson.*"Constrained Capacities for Faster-Than-Nyquist Signaling"*. Information Theory, IEEE Trans, vol. 55, no. 2, pp. 764-775, Feb. 2009.

[12] D. Dasalukunte, F. Rusek and J.B. Anderson.*"Transmitter architecture for Faster-Than-Nyquist signaling systems"*. In Circuits and Systems, 2009. ISCAS 2009. IEEE International Symposium, pp. 1028-1031, May. 2009.

[13] D. Dasalukunte, F. Rusek, V. Owall. *"An Iterative Decoder for Multicarrier Faster-Than-Nyquist Signaling Systems"*. In Communication (ICC), 2010. IEEEE International Conference, pp. 1-5, May. 2010.

[14] H. Lin, N. Lahbabi, P. Siohan and X. Jiang. *"An efficient FTN Implementation of the OFDM/OQAM System"*. In Communication (ICC), 2015. IEEEE International Conference, pp. 4787-4792, June. 2015.

[15] M. Bellanger. *"Specification and design of a prototype filter for filter bank multicarrier transmission"*. ICASSP, 2001.